Comparison of density functionals for energy and structural differences between the high- $[^5T_{2g}:(t_{2g})^4(e_g)^2]$ and low- $[^1A_{1g}:(t_{2g})^6(e_g)^0]$ spin states of iron(II) coordination compounds. II. More functionals and the hexaminoferrous cation, $[Fe(NH_3)_6]^{2+}$

Antony Fouqueau and Mark E. Casida[a)]
Institut de Chimie Moléculaire de Grenoble (ICMG, FR-2607), Équipe de Chimie Théorique, Laboratoire d'Études Dynamiques et Structurales de la Sélectivité (LEDSS), UMR CNRS/UJF 5616 Université Joseph Fourier (Grenoble I), F38041 Grenoble, France

Latévi Max Lawson Daku and Andreas Hauser
Département de Chimie Physique, Université de Genève, 30 quai Ernest-Ansermet, CH-1211 Genève 4, Switzerland

Frank Neese
Max Planck Institute für Bioanorganische Chemie, Stiftstrasse 34-36, Mülheim an der Ruhr 45470, Germany

(Received 22 July 2004; accepted 4 November 2004; published online 7 January 2005)

The ability of different density functionals to describe the structural and energy differences between the high- $[^5T_{2g}:(t_{2g})^4(e_g)^2]$ and low- $[^1A_{1g}:(t_{2g})^6(e_g)^0]$ spin states of small octahedral ferrous compounds is studied. This work is an extension of our previous study of the hexaquoferrous cation, $[Fe(H_2O)_6]^{2+}$, [J. Chem. Phys. **120**, 9473 (2004)] to include a second compound—namely, the hexaminoferrous cation, $[Fe(NH_3)_6]^{2+}$—and several additional functionals. In particular, the present study includes the highly parametrized generalized gradient approximations (GGAs) known as HCTH and the meta-GGA VSXC [which together we refer to as highly parametrized density functionals (HPDFs)], now readily available in the GAUSSIAN03 program, as well as the hybrid functional PBE0. Since there are very few experimental results for these molecules with which to compare, comparison is made with best estimates obtained from second-order perturbation theory-corrected complete active space self-consistent field (CASPT2) calculations, with spectroscopy oriented configuration interaction (SORCI) calculations, and with ligand field theory (LFT) estimations. While CASPT2 and SORCI are among the most reliable *ab initio* methods available for this type of problem, LFT embodies many decades of empirical experience. These three methods are found to give coherent results and provide best estimates of the adiabatic low-spin–high-spin energy difference, $\Delta E_{LH}^{\text{adia}}$, of 12 000–13 000 cm^{-1} for $[Fe(H_2O)_6]^{2+}$ and 9 000–11 000 cm^{-1} for $[Fe(NH_3)_6]^{2+}$. All functionals beyond the purely local approximation produce reasonably good geometries, so long as adequate basis sets are used. In contrast, the energy splitting, $\Delta E_{LH}^{\text{adia}}$, is much more sensitive to the choice of functional. The local density approximation severely over stabilizes the low-spin state with respect to the high-spin state. This "density functional theory (DFT) spin pairing-energy problem" persists, but is reduced, for traditional GGAs. In contrast the hybrid functional B3LYP underestimates $\Delta E_{LH}^{\text{adia}}$ by a few thousands of wave numbers. The RPBE GGA of Hammer, Hansen, and Nørskov gives good results for $\Delta E_{LH}^{\text{adia}}$ as do the HPDFs, especially the VSXC functional. Surprisingly the HCTH functionals actually over correct the DFT spin pairing-energy problem, destabilizing the low-spin state relative to the high-spin state. Best agreement is found for the hybrid functional PBE0. © *2005 American Institute of Physics.* [DOI: 10.1063/1.1839854]

I. INTRODUCTION

The identification of the spin symmetry of the ground and low-lying excited states is important for the comprehension of chemical reactivity. However, many interesting cases occur, especially among transition metal coordination compounds, where the competition between the splitting of nearly degenerate orbitals with the electron pairing energy makes the prediction of relative spin-state energetics difficult at best. Our own interest is in the spin-crossover phenomenon in transition metal coordination complexes and its use in making molecular switches. A recent review of this area may be found in Ref. 1, while Refs. 2, 3 provide older reviews. The difficulty of carrying out high quality *ab initio* calculations for transition metal coordination compounds, combined with the desire to go beyond simple ligand field theory, has pushed several workers to make a detailed examination of density functional theory (DFT) for the prediction

[a)]Electronic mail: Mark.Casida@ujf-grenoble.fr

of relative spin-state energetics.[4–10] Much of this work is described in a recent review of Harvey.[9] The focus has frequently been on the comparison of DFT calculations with experimental results for medium- and large-sized compounds. So far, our own contribution to this area has been a detailed comparison of DFT calculations with ligand field and *ab initio* results for the relatively small "textbook example" of $[Fe(H_2O)_6]^{2+}$ (Ref. 8). Although experimental data is often only available indirectly for such small compounds through ligand field parameters, we believe that the ability to compare with the results of *ab initio* calculations, even if far from trivial, without having to worry about additional factors such as vibrational and environmental effects typically present in experimental data, provides a valuable complement to previous assessments of density functionals for larger compounds. In this paper, we extend our previous work to several different functionals which have only recently become widely available as well as to a second simple compound, $[Fe(NH_3)_6]^{2+}$, with a larger ligand field splitting than in $[Fe(H_2O)_6]^{2+}$.

Our paper is divided into the following sections. A review of the different functionals used in this study is given in the following section. Ligand field estimations are given in Sec. III. The technical details and the results of our *ab initio* reference calculations are given in Sec. IV. In Sec. V, we give our DFT results. We give first the computational details, then, we consider optimized geometries, and then, we give a comparison of HS and LS complex energies. Sec. VI summarizes.

II. DENSITY FUNCTIONALS AND THE PAIRING-ENERGY PROBLEM

An important goal of this paper is the comparison of the relative ability of density functionals to treat different spin states. This may be termed the "DFT pairing-energy problem." Although this name is particulary appropriate when considering applications to transition metal coordination complexes, the problem is of course a more general one. This section introduces the DFT pairing-energy problem and provides a brief review of the different exchange-correlation (xc) functionals used in the present study.

Almost all applications of DFT are based on the Kohn-Sham formalism[11] and our work is no exception. It is now common practice to use the spin-density variant.[12] The different approximations considered here differ by the form of the exchange correlation energy E_{xc}.

The traditional workhorse of DFT is the local density approximation (LDA), where the xc energy density at each point $\mathbf{r}$ is approximated by the xc energy density of a homogeneous electron gas whose densities ρ_σ are identical to the local densities $\rho_\sigma(\mathbf{r})$. We have used the Vosko-Wilk-Nussair (VWN) parametrization of the Ceperley-Alder quantum Monte-Carlo calculations[13] (This is the VWN5 option in GAUSSIAN03, *not* the VWN option). The LDA works much better than might be expected, given that molecular densities are not at all homogeneous. Part of the explanation is that the LDA works by error compensation: a small ($\sim$14%) underestimation of the exchange energy is compensated by a large ($\sim$250%) overestimation of the correlation energy.[14] This is often good enough for such properties as molecular geometries and vibrational frequencies.[15]

In contrast, an accurate treatment of exchange effects would seem of critical importance when comparing energies of different spin states. According to a common textbook explanation of Hund's rule,[16] exchange effects favor high-spin states by keeping parallel spin electrons separated, thereby minimizing electron repulsion. We have pointed out that this reasoning is heuristic, not rigorous.[8] Nevertheless it suggests that the underestimation of exchange in the LDA should lead to an artificial destabilization (stabilization) of high-(low) spin states relative to low-(high) spin states. This is the DFT pairing-energy problem and it is by no means limited to just the LDA.[8,9]

A well-known problem of the LDA is that it seriously overestimates molecular bond energies. Early attempts at correcting the LDA by introducing gradient-correction terms were largely unsuccessful until the development of generalized gradient approximations (GGAs) in the 1980s. One of the most successful GGAs has been Becke's 1988 exchange-only GGA (B) which has the proper asymptotic limit for ϵ_{xc}.[17] It contains a single parameter whose value was obtained by fitting to the Hartree-Fock exchange energies of the noble gases. An example of a GGA correlation functional is that of Lee, Yang, and Parr (LYP).[18] Acronyms for xc functionals obtained by combining exchange-only functionals and correlation-only functionals are generated by simply concatenating the acronyms of the separate functionals (e.g. B+LYP$\rightarrow$BLYP).

Further improvement was obtained in the 1990s by the use of hybrid functionals which consist of linear combinations of exact (i.e., Hartree-Fock) exchange and GGAs. The justification for such an approach was presented by Becke[19] using the adiabatic connection formalism of Harris and Jones.[20] Becke proposed the B3PW91 hybrid functional,

$$E_{xc}=E_{xc}^{\mathrm{LDA}}+a_0(E_x^{\mathrm{HF}}-E_x^{\mathrm{LDA}})+a_xE_x^{B88}+a_cE_c^{PW91}, \quad (2.1)$$

where a_0, a_x, and a_c are semiempirical coefficients obtained by fitting to experimental data[21] (the "3" in B3PW91 refers to the presence of three semiempirical parameters). Becke's parameters have been used without reoptimization, in the popular B3LYP functional.[22] More recently, and in keeping with their *ab initio* philosophy, Perdew, Burke, and Erznerhof provided an *ab initio* estimate of the hybrid mixing parameter.[23] This had been incorporated into the zero-parameter PBE functional (PBE0).[23,24]

Previous work applying DFT to spin crossover and related problems made use of pre-1995 functionals. (An exception is Reihers's work[5] which also mentions calculations with the PBE and PBE0 functional.) All GGAs were found to suffer from the DFT spin pairing problem, although less so than does the LDA.[4–7] In contrast the B3LYP functional appeared to over stabilize the HS state because of the presence of too much HF exchange. Depending on the functional, DFT frequently gave the wrong ground-state spin symmetry in comparison with experiment. This suggested that a pragmatic solution to the problem would be to retune the a_0 mixing parameter in the B3LYP functional so as to minimize

TABLE I. Summary of functionals used in the present study.

Functional	Year	Citation	Type	
$X\alpha$	1951	64	Local	Exchange only
LDA	1980[a]	11	Local	Exchange correlation
P86	1986	77	GGA	Correlation only
B	1988	17	GGA	Exchange only
LYP	1988	18	GGA	Correlation only
PW91	1991	78	GGA	Exchange correlation
B3LYP	1994	22	Hybrid	Exchange correlation
PBE	1996	23	GGA	Exchange correlation
RPBE	1998	79	GGA	Exchange correlation
HCTH93	1998	30	GGA	Exchange correlation
HCTH107	1998	30	GGA	Exchange correlation
HCTH407	1998	30	GGA	Exchange correlation
VSXC	1998	29	Meta-GGA	Exchange correlation
PBE0	1999	24	Hybrid	Exchange correlation
B3LYP*	2002	5	Hybrid	Exchange correlation

[a]VWN parametrization (Ref. 13).

the DFT pairing energy problem. The result is the B3LYP* functional with 15% HF exchange.[5–7] The same approach has been used before to reoptimize the B3LYP functional for other sensitive properties. The result is unfortunately property dependent, being 30% HF exchange for excitation energies[25] and 5% HF exchange for NMR chemical shifts.[26] So this is certainly not a universal solution. Another criticism of previous DFT work applied to spin-crossover systems is that the comparison has always been between calculated properties of gas phase molecules with experimental values obtained from condensed phase measurements. Environmental effects on spin crossover can be huge since the high-spin/low-spin difference in the metal bond length is on the order of 0.2 Å. Dramatic changes in spin-crossover behavior in crystals have even been observed just by varying the intercalated solvent.[27] This is why we prefer in this and our previous work[8] to compare results from DFT with the results of good *ab initio* calculations for gas phase molecules.

Much improved GGAs have become readily available since the previous work on spin crossover. Furthermore there are drawbacks to Hartree-Fock exchange. It can be expensive to calculate compared to a pure GGA (depending upon the size of the system and skill of the programmer) and is known to give qualitatively incorrect results for systems, such as transition metal complexes, where there are a number of low-lying virtual orbitals. Highly parametrized density functionals (HPDFs) provide an alternative to hybrid functionals at the cost of a large number of parameters to optimize. In one approach to making a HPDF, Voorhis and Scuseria[28] developed a Taylor series-like density matrix expansion to obtain the so-called VSXC exchange-correlation functional[29] which has 21 parameters. It is in fact a meta-GGA, since it depends not only on the density and its gradients but also on the orbital-dependent local kinetic energy density τ. In another approach, Hamprecht, Cohen, Tozer, and Handy[30] developed a series of HPDFs whose 15 parameters were fit simultaneously to experimental data and to *ab initio* xc potentials. The resultant HCTH93, HCTH147, and HCTH407 are distinguished by the number of molecules (93, 147, or 407) in the parameter training set. The HPDFs often do as well as, if not better than, previous hybrid functionals. They are included in the present assessment of density functionals for application to spin-crossover systems. All the functionals used in this work are reported in Table I.

III. LIGAND FIELD THEORY

High-spin–low-spin bond length differences,

$$\Delta r_{HL} = r_{HS} - r_{LS}, \tag{3.1}$$

may be estimated using a simple model described by Figgis and Hitchmann (Ref. 31 p. 146). Although not used for this purpose by Figgis and Hitchmann, the model can also be used to estimate the adiabatic energy difference,

$$\Delta E_{LH}^{\text{adia}} = E_{LS}(r_{LS}) - E_{HS}(r_{HS}). \tag{3.2}$$

This model is briefly reviewed here for application in the present context.

We assume strictly octahedral $[FeL_6]^{2+}$ with Fe–L distance r_{LS} in their LS $[^1A_{1g}:(t_{2g})^6(e_g)^0]$ state and r_{HS} in their HS $[^5T_{2g}:(t_{2g})^4(e_g)^2]$ state. Of course, the HS state is electronically degenerate in O_h symmetry and so will Jahn-Teller distort, but we presume that the distortion is small enough to be neglected. Since H_2O and NH_3 are relatively weak ligands, the spin pairing energy exceeds the ligand field splitting,

$$\Delta = \epsilon(e_g) - \epsilon(t_{2g}), \tag{3.3}$$

so that the ground-state configuration is HS. The HS→LS excitation energy at fixed r is

$$\Delta E_{LH}(r) = E_{LS}(r) - E_{HS}(r) = -m\Delta(r) + S, \tag{3.4}$$

where

$$m = 2 \tag{3.5}$$

is the number of electrons deexcited from the e_g to the t_{2g} orbitals and the spin pairing energy S is assumed independent of r. Thus the vertical excitation energy is (Fig. 1)

$$\Delta E_{LH}^{\text{vert}} = \Delta E_{LH}(r_{HS}). \tag{3.6}$$

Two approximations allow us to express $\Delta E_{LH}^{\text{adia}}$ in terms of $\Delta E_{LH}^{\text{vert}}$. The first is the harmonic approximation for the breathing mode of the HS state,

$$E_{HS}(r) = E_{HS}(r_{HS}) + \frac{N}{2} k_{HS}(r_{HS} - r)^2, \tag{3.7}$$

where k_{HS} is the breathing mode force constant and $N=6$ is just the number of ligands. The second approximation is for the geometry dependence of the ligand field splitting. From various considerations (see Ref. 31 pp. 39 and 69),

$$\Delta(r) = \Delta_{HS}\left(\frac{r}{r_{HS}}\right)^{-n}, \tag{3.8}$$

where typically $5 < n < 6$, with $n \cong 5$ being a reasonable choice. Expanding

$$\left(1 + \frac{r - r_{HS}}{r_{HS}}\right)^{-n} = 1 - n\frac{r - r_{HS}}{r_{HS}} + \frac{n(n+1)}{2}\left(\frac{r - r_{HS}}{r_{HS}}\right)^2 + \cdots, \tag{3.9}$$

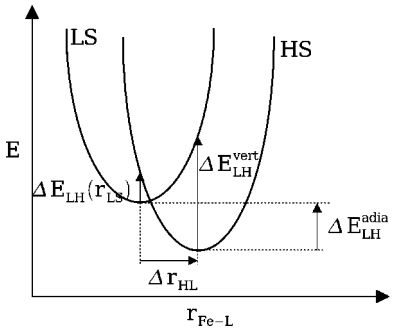

FIG. 1. Representation of the potential wells for the quintet and singlet states with the different quantities cited in the text.

and truncating to linear order gives the expression actually used in the model, namely,

$$\Delta(r) \approx \Delta_{HS}\left(1 + n\frac{r_{HS}-r}{r_{HS}}\right). \tag{3.10}$$

The two aforementioned approximations lead to

$$\begin{aligned} E_{LS}(r) - E_{HS}(r_{HS}) &= \Delta E_{LH}(r) + \frac{N}{2}k_{HS}(r_{HS}-r)^2 \\ &= -m\Delta(r) + S + \frac{N}{2}k_{HS}(r_{HS}-r)^2 \\ &= -m\left(1 + n\frac{r_{HS}-r}{r_{HS}}\right)\Delta_{HS} + S + \frac{N}{2}k_{HS}(r_{HS}-r)^2. \end{aligned} \tag{3.11}$$

Minimizing with respect to r leads to

$$\Delta r_{HL} = \frac{nm}{N}\frac{\Delta_{HS}}{k_{HS}r_{HS}}. \tag{3.12}$$

This formula is known to work well in a number of cases (Ref. 31, Table 7.1, p. 147). For $r = r_{LS}$ in Eq. (3.11), we obtain the formula for the adiabatic excitation energy

$$\Delta E_{LH}^{\text{adia}} = \Delta E_{LH}^{\text{vert}} - \frac{N}{2}k_{HS}(\Delta r_{HL})^2. \tag{3.13}$$

Note that there is something clearly disturbing about this latter formula since it implies the same force constant for the LS state as for the HS state [see Eq. (3.11)]. This is a consequence of keeping no more than linear terms in the expansion of $\Delta(r)$. Keeping quadratic terms leads to unphysical result that $k_{LS} < k_{HS}$ and results in an even more serious degradation of calculated Δr_{HL} when compared with experiment.

These equations are practical and reasonably reliable. The reliability of the equations comes from decades of LFT experience.[31] They are practical because geometric quantities such as k_{HS} and r_{HS} are measurable or (as we shall see) relatively easy to calculate. The ligand field splitting may be estimated as $\Delta(r_{HS}) = fg$ using tabulated data for f and g. The vertical excitation energy $\Delta E_{LH}^{\text{vert}}$ may be determined from the appropriate Tanabe-Sugano diagram and appropriate values of the Racah parameters B and C Racah parameters: LFT estimations very much depend upon which Tanabe-Sugano diagram one takes. The one most often reproduced in the literatures sets $C/B = 4.8$ which according to Tanabe and Sugano is the correct ratio for Co(III). We use the ratio 4.41 which according to Tanabe and Sugano is more appropriate for Fe(II). This diagram is the one we can find in the book by Figgis and Hitchman.[31] Then, we have to choose the value to take for B: Figgis give $B = 1080\ \text{cm}^{-1}$ with $C/B = 4.42$, Tanabe-Sugano[32] give $B = 917\ \text{cm}^{-1}$ with $C/B = 4.41$, Griffith[33] gives $B = 1058\ \text{cm}^{-1}$ with $C/B = 3.69$, and Schäfer[34] gives $B = 897\ \text{cm}^{-1}$ with $C/B = 4.3$. Then, we have to reduce the value of B by an orbital reduction factor β. In order to stay consistent, we choose to take all values and Tanabe-Sugano diagram as given by Figgis and Hitchman. The results are quantitatively quite useful but the presence of rough approximations at some steps emphasizes the desirability of a more rigorous model.

Input parameters and calculated Δr_{HL} and $\Delta E_{HL}^{\text{adia}}$ are given in Table II for the two molecules treated in this paper.

IV. *AB INITIO* REFERENCE CALCULATIONS

Our objective is to assess the relative performance of different density functionals for calculation of the properties of small Fe(II) octahedral coordination complexes by direct comparison with zero-temperature gas phase nonrelativistic *ab initio* quantum chemistry calculations of the highest possible quality, in the sense that they are at the limit of what is currently computationally feasible. We have carried out such calculations using two different computational methods, namely, (i) the well-established method of complete active space (CAS) (Ref. 35) multiconfiguration self-consistent field (SCF) calculations with and without second-order perturbation theory (PT2) corrections[36,37] and (ii) spectroscopy oriented configuration interaction (SORCI) (Ref. 38) calculations based on the difference dedicated configuration interaction (DDCI) method of Malrieu and co-workers.[39,40] There is an extensive experience with CASPT2 calculations and its strengths and limitations are now well known.[41] In particular, as will be made clear below, the size of the CAS grows rapidly as new orbitals are included, so that only a limited number of orbitals may be included in the CAS. Furthermore the inclusion of dynamical correlation at the PT2 level is often insufficient for $3d$ transition metal complexes, partly because of practical difficulties using very large basis sets and partly because of the restriction to second order in the perturbation theory. The deficiencies are countered by the use of empirical "atomic corrections." In principle, the DDCI approach used in the SORCI method allows the accurate calculation of differential dynamical correlation with a smaller number of configurations. The SORCI method is relatively different and so necessarily less well characterized, though all indications are that it works well.

A. CASSCF and CASPT2 calculations

1. Computational details

Our CASSCF and CASPT2 calculations were carried out with the program MOLCAS.[42] The orbital basis sets used were of 6-31G** quality.[43,44] This corresponds to basis D in pa-

per I, which was the largest basis set (178 functions) for which we could perform CASPT2 calculations on the computers available to us. The choice of the active space was governed by the desire to include a maximum of orbitals in the CAS while keeping the calculations down to a practical size. In particular, we have accounted for the so-called "$3d$ double shell effect" [45–47] which says that the inclusion in the CAS of all molecular orbitals containing significant metal $3d$ contributions is critical for describing the large radial correlation effects present in the type of complex being studied here. This means that the CASSCF performs a full CI calculation on 12 electrons distributed over 10 orbitals, denoted CASSCF (12,10) and CASPT2 (12,10). See paper I for additional details regarding the choice of active space. Automatic structure optimization and frequency calculations (to confirm minima) were carried out at the CASSCF level. This was not possible at the CASPT2 level where only single point calculations were performed. As already mentioned, although we have carried out CASSCF and CASPT2 calculations close to the limit of what we can do on the computers available to us, such calculations are known to require an empirical atomic correction for missing dynamical correlation.[8,48] This correction which is described in greater detail in paper I, assumes that the missing correlation is primarily localized on the iron atom and so may be estimated by comparing CASPT2 calculations space and orbital basis set with known experimental excitation energies. The HS-LS energy difference is calculated as (paper I)

$$\Delta E_{LH}^{\text{shifted}} = \Delta E_{LH}^{\text{direct}} + (\Delta E_{\text{atom}}^{\text{expt}} - \Delta E_{\text{atom}}^{\text{calc}}). \tag{4.1}$$

2. Results

The necessary *ab initio* calculations are far from trivial. An often cited objective for "chemical accuracy" is 1 kcal/mol ($350\ \text{cm}^{-1}$), but errors of 5 kcal/mol ($1\,750\ \text{cm}^{-1}$) are more typical in good *ab initio* calculations.[49,50] Electron correlation is especially difficult to treat in compounds containing $3d$ transition metals such as Fe. In our earlier work,[8] our best estimate of the true (i.e., complete CI) value of $\Delta E_{LH}^{\text{adia}}$ for $[\text{Fe}(\text{H}_2\text{O})_6]^{2+}$ were $12\,350\ \text{cm}^{-1}$, based upon a CASPT2 calculation with a $3\,000\ \text{cm}^{-1}$ atom-based empirical shift[8] (labeled CASPT2corr) needed to include important dynamic correlation effects not present in the CASPT2 calculation, and $13\,360\ \text{cm}^{-1}$, obtained by the SORCI method with its difference-dedicated CI philosophy.[39,40] The same strategy applied to $[\text{Fe}(\text{NH}_3)_6]^{2+}$ in the context of the present work gives $9\,120\ \text{cm}^{-1}$ from CASPT2 with the atom-based empirical shift.

B. SORCI calculations

1. Computational details

SORCI calculations were carried out with the ORCA package[51] at the B3LYP/TZVP optimized geometries. The SORCI method is a combination of several different many-body techniques. It is described in detail in Ref. 38. We confine ourselves here to recalling some of the basic steps taken during the calculation and to defining the basis sets and thresholds that we used.

TABLE II. Parameters entering into and results of the simple model described in the text. Experimental data and corresponding results are given in parentheses.

	LFT parameters	
	$[\text{Fe}(\text{NH}_3)_6]^{2+}$	$[\text{Fe}(\text{H}_2\text{O})_6]^{2+}$
	From LFT	
Δ_{HS}[a]	$12\,500\ \text{cm}^{-1}$	$10\,000\ \text{cm}^{-1}$
$\Delta E_{LH}^{\text{vertb}}$	$9200\ \text{cm}^{-1}$	$15\,500\ \text{cm}^{-1}$
	From DFT[c]	
ν_{HS}	$304\ \text{cm}^{-1}$	$344\ (379)\ \text{cm}^{-1}$[d]
r_{HS}	2.260 Å	2.126 (2.12) Å[e]
	Results	
k_{HS}	$0.93\times10^5\ \text{dyn cm}^{-1}$	$1.26\times10^5\ (1.5\times10^5)\ \text{dyn cm}^{-1}$
Δr_{HL}	0.198 Å	0.126 (0.11) Å
$\Delta E_{LH}^{\text{adia}}$	$5000\ \text{cm}^{-1}$	$12\,000\ (12\,500)\ \text{cm}^{-1}$

[a]$\Delta_{HS}=fg$ (f and g are tabulated, see, e.g., Ref. 31, P. 219).
[b]From the d^6 Tanabe-Sugano diagram and appropriate values of the Racah parameters B and C (see text).
[c]These are averages quantities over several DFT results.
[d]From Ref. 80.
[e]Averaged over known structures.

Two relatively extensive basis sets were used in the calculations. Basis C (312 functions) consists of the triple-ζ (TZV) basis of Schäfer *et al.*[52] augmented with one set of p-functions for H ($5s1p$ contracted to $3s1p$; 311/1) and two sets of d-functions for N (11s6p2d contracted to $5s3p2d$; 62111/411/11) with polarization exponents taken from the TURBOMOLE library. [Basis sets were obtained from the file transfer protocol (ftp) server of the quantum chemistry group at the University of Karlsruhe (Germany) under ftp://ftp.chemie.uni-karlsruhe.de/pub/basen]. The metal in Basis C is described by the Wachters basis[53] with two sets of p-type polarization functions and three f-sets contracted in a 2,1 fashion by Bauschlicher *et al.*[54] ($14s11p6d3f$ contracted to $8s6p4d2f$; 62111111/331211/3111/21). The second basis set (Basis D, 423 functions) is more extensive and features a second set of p-polarization functions on H and an additional f-set for N (TZVPP) basis. The metal is described by the recently developed quadruple-ζ[55] quality basis of the Ahlrichs group which already contains diffuse p and d sets and is augmented with three sets of f-polarization functions (QZVP, the g-function in the original QZVP basis was deleted; $24s18p10d3f$ contracted to $11s6p5d3f$; 11,411111111/951111/61111/111). The fitting basis for the resolution of the identity (RI) approximation used in the ORCA correlation package where those developed for RI-MP2 by Weigend *et al.*[56] and in the case of the QZVP iron basis was taken from unpublished work in the TURBOMOLE library. For technical reasons h and i functions contained in this fit basis had to be deleted.

A simplified flow diagram of the SORCI algorithm is given in Fig. 2. The first step is to construct a set of occupied and virtual orbitals whose configurations define an initial reference space S_0. This was done starting from spin-averaged Hartree-Fock orbitals[57] with six electrons in the five iron d-based molecular orbitals. The virtual orbitals were improved by diagonalizing a $N-1$ electron Fock operator in

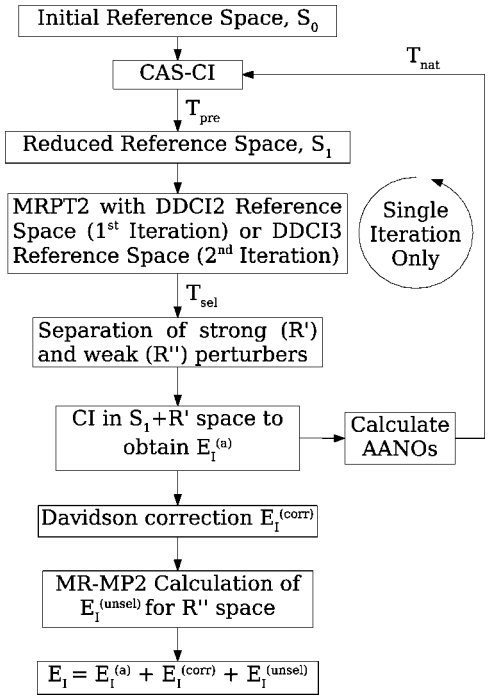

FIG. 2. Diagram of the SORCI algorithm (based on Fig. 1 of Ref. 38), showing the principle steps and the three thresholds, T_{pre}, T_{nat}, and T_{sel}.

the virtual space where the additional hole is smeared out over all occupied orbitals participating in the correlation calculation.[58] Since the core orbitals with energies less than $-5\ E_h$ ($E_h=1$ hartree) were frozen this amounts to the full valence space. No virtual orbitals were neglected in the correlation calculations.

In the following step the orbital space is partitioned into internal, active, and external (virtual) MOs, and a CAS-CI calculation is performed in the active space [in the present case, this is a CAS(6,5)]. From this small CI the configurations with a weight exceeding the threshold value T_{pre} (10^{-4} in this study) are selected and the Hamiltonian is diagonalized again in the reduced reference space to give the zeroth-order multiconfigurational many electron wave functions $|0\rangle$ and energies E_0 for each state of interest.

This is followed by second-order Møller-Plesset perturbation theory within a restricted set of excited configurations, namely, within a difference-dedicated configuration interaction (DDCI) set. The density corresponds to the zeroth-order states used to define a spin-averaged Fock-type operator, the diagonal elements of which are used to define orbital energies which are used in the diagonal definition of the zeroth-order Hamiltonian

$$\hat{H}_{0,diag}=\sum_p \epsilon_p \hat{a}_p^+ \hat{a}_p \tag{4.2}$$

(details are found in Refs. 59, 60). The program proceeds by constructing the properly spin-coupled single and double excitations $|I\rangle$ relative to each individual reference configuration in $|0\rangle$. Configurations are sorted into the weakly and strongly interacting subspaces according to the diagonal second-order energy estimate, i.e., configuration state functions (CSFs) with

$$|\langle 0|\hat{H}|I\rangle|^2(\langle I|\hat{H}_{0,\mathrm{diag}}|I\rangle-\langle 0|\hat{H}_{0,\mathrm{diag}}|0\rangle)^{-1}\geqslant T_{\mathrm{sel}} \tag{4.3}$$

are part of the strongly interacting subspace R' and the remaining CSFs are part of the weakly interacting subspace R'' ($\hat{H}$ is the full Born-Oppenheimer Hamiltonian). The threshold T_{sel} was set as $10^{-6}\ E_h$ in this study. After the selection step, which is initially carried out in the difference-dedicated CI "2" (DDCI2) subspace of the first-order interacting space, the $R'+S_1$ space is diagonalized. This makes the method immune to intruder states and includes the electronic relaxation of the reference wavefunction in the dominant part of the "correlation field."

The resulting CI first-order densities are averaged over all states of interest and the approximate average natural orbitals (AANOs) with significant occupations (according to a third threshold T_{nat} set to 10^{-5} in this study) are produced for the second step of the procedure. This second step is a selected DDCI3 calculation in the AANO basis.

The CI energies after this second step are corrected for higher than double excitations using the approximate multireference Davidson correction,[61,62] E_I^{corr}, and the energetic effect of the R'' space, E_I^{unsel}, is calculated with diagonal MR-MP2 theory as described above using the relaxed reference part of the final DDCI3 wave function.

2. Results

SORCI calculations were carried out for the B3LYP/TZVP HS and LS optimized structures with the two relatively extensive basis sets *C* and *D*. The larger basis set *D* leads to a further increase in transition energies by $\sim 1000\ \mathrm{cm}^{-1}$ compared to the already rather flexible basis *C* (Table III).

Since SORCI does not lend itself well to the calculation of adiabatic transition energies due to the neglect of inactive double excitations, some estimate of the relaxation energy for each electronic state needs to be provided. At the B3LYP/TZVP level the relaxation energy for the HS state was found to be $6488\ \mathrm{cm}^{-1}$ while that of the low-spin state was calculated to be $5083\ \mathrm{cm}^{-1}$. If these numbers are combined with the SORCI results for the vertical transition energy in order to arrive at an estimate of the adiabatic transition energy, two equivalent cycles [leading to estimates $\Delta E_{LH}^{\mathrm{adia}}(1)$ and $\Delta E_{LH}^{\mathrm{adia}}(2)$] can be conceived which would lead to identical results if all energies would be calculated with the same method and basis set,

$$\begin{aligned}\Delta E_{LH}^{\mathrm{adia}}(1)&=\Delta E_{LH}^{\mathrm{vert}}(HS)-\Delta E_{LH}^{\mathrm{relax}}(LS),\\ \Delta E_{LH}^{\mathrm{adia}}(2)&=\Delta E_{LH}^{\mathrm{vert}}(LS)+\Delta E_{LH}^{\mathrm{relax}}(HS).\end{aligned} \tag{4.4}$$

Here $\Delta E_{LH}^{\mathrm{vert}}(HS)$ and $\Delta E_{LH}^{\mathrm{vert}}(LS)$ are the vertical transition energies at the optimized HS and LS geometries, respectively, and $\Delta E_{LH}^{\mathrm{relax}}(LS)$ and $\Delta E_{LH}^{\mathrm{relax}}(HS)$ are the relaxation energies for the low-spin and and high-spin states, respectively. They are defined as the energy of the low-spin state at the high-spin geometry minus the energy of the low-spin state at the low-spin geometry and equivalently for the high-spin state. The results are summarized in Table III. The entry $\Delta E_{LH}^{\mathrm{adia}}(\mathrm{SORCI})$ is the straightforward adiabatic energy from

TABLE III. Vertical and adiabatic transition energies calculated with the SORCI method for the $[Fe(NH_3)_6]^{2+}$ complex at the B3LYP/TZVP optimized HS and LS geometries.

	Vertical transition energies (cm^{-1})		Adiabatic transition energies (cm^{-1})		
Basis	ΔE_{LH}^{vert}(HS)	ΔE_{LH}^{vert}(LS)	$\Delta E_{LH}^{adia}(1)$	$\Delta E_{LH}^{adia}(2)$	ΔE_{LH}^{adia}(SORCI)
C	16 635	5455	10 247	10 538	11 278
D	17 780	6315	11 293	11 398	13 277

SORCI calculations which do not take any inactive double excitation into account and should therefore be viewed with caution.

In general, the results are pleasingly consistent in the sense that $\Delta E_{LH}^{adia}(1)$ and $\Delta E_{LH}^{adia}(2)$ differ only by $\sim 200\ cm^{-1}$ which is within the uncertainty of the method. The results for basis *C* and basis *D* differ by $\sim 1000\ cm^{-1}$ and we conclude that the best estimate of the adiabatic transition energy from SORCI is $\sim 11\,000\ cm^{-1}$, which is in reasonable agreement with the empirically corrected CASPT2 calculations.

V. VALIDATION OF DENSITY FUNCTIONALS

The quality of approximate density functionals for xc energy has gradually improved since the introduction of the local density approximation by Kohn and Sham[11] (some would say, since the exchange functional of Dirac[63] and subsequent $X\alpha$ approximation[64]). This improvement seemed to have accelerated since the introduction of GGAs in the 1980s and of hybrid functionals in the 1990s. It is now *de rigueur* for the functionals to be tested against the popular G*n* ($n=1,2,3$) sets of comparison data.[65–68] However this is a necessary, but not a sufficient, test of the general validity of an xc functional. The G*n* sets are notoriously weak in test data for compounds containing transition metals. The G*n* test sets also tend to be heavily weighted towards ''normal'' covalent-type bonding. Our interest is in the relative geometries and energetics of transition metals complexes in different spin states. In this section we present results extending our previous work[8] on $[Fe(H_2O)_6]^{2+}$ to several new functionals and present results for $[Fe(NH_3)_6]^{2+}$, a compound not previously considered but which brings us (arguably) closer to the FeN_6 configuration often seen in Fe(II) spin-crossover compounds.[3]

A. Computational details

The DFT calculations reported here were carried out with GAUSSIAN,[69] ORCA,[51] and ADF.[70] These programs differ in several respects, among the algorithmic differences, the most important is certainly that GAUSSIAN and ORCA use basis sets of Gaussian-type orbitals (GTOs) while ADF uses Slater-type orbital (STO) basis sets. These two types of basis sets behave rather differently and it is difficult to say *a priori* which GTO and STO basis sets should be of comparable quality, though calculations carried out with identical functionals and the two types of basis sets permit a rough correspondence to be made. This was done in Sec. IV C of paper I where it was pointed out that the TZ2P STO basis gave results comparable to those obtained with a TZVP GTO basis set. The basis sets used in this study are summarized in Table IV.

At the SCF level, convergence to the wrong electronic state was less frequently encountered than in the previous study with the previous version of GAUSSIAN.[71] This problem has apparently been overcome by different convergence algorithms and, in particular, the more robust fractional occupation convergence algorithm.[72,73]

B. Optimized geometries

We first consider the geometrical structures of the free gas phase cations. As remarked in our earlier work,[8] available comparison data does not allow us to make fine distinction between $[Fe(H_2O)_6]^{2+}$ geometries optimized using different density functionals. This is partly because all functionals beyond the LDA level (except perhaps the RPBE functional) give relatively good geometries and partly because available experimental data is for crystals where cation structure is heavily influenced by (among other things) the nature of the counter ions. The same observation may be made for $[Fe(NH_3)_6]^{2+}$. We thus focus on identifying trends among geometries obtained using various functionals.

Both $[Fe(H_2O)_6]^{2+}$ and $[Fe(NH_3)_6]^{2+}$ are octahedral complexes. According to the simple LFT model, the HS electronic state is degenerate in O_h symmetry. We should therefore expect a Jahn-Teller distortion. As evidenced by our earlier work,[8] this effect is small in $[Fe(H_2O)_6]^{2+}$. In $[Fe(NH_3)_6]^{2+}$, the axial Fe–N bonds are found to be only about 0.020 Å longer than the equitorial Fe–N bonds in calculations with our more complete basis sets (*B* or *C*″). A superposition of HS and LS geometries is shown in Fig. 3. Figure 3 of Ref. 8 shows a superposition of HS and LS geometries for $[Fe(H_2O)_6]^{2+}$.

Since the Jahn-Teller distortion is small, we will focus on average iron-ligand bond lengths. These bond lengths depend somewhat on the choice of basis set used for the calculation. Our $[Fe(NH_3)_6]^{2+}$ calculations were carried out with the 6-31G** basis set (*A*) and the more flexible TZVP basis set of Ahlrichs (*B*). Figure 4 shows that the bond length differences also depend upon the functional, with bond lengths being longer for basis set *B* than for basis set *A*. The inverse trend for basis *A*″ and *C*″ is observed for calculations with ADF but it must be kept in mind that these STO bases are not the same as the GTO bases. Basis set convergence for $[Fe(H_2O)_6]^{2+}$ geometries has been discussed in our earlier work.[8] Most importantly, the value of Δr_{HL} (~ 0.20 Å) is relatively large compared to variations

TABLE IV. Summary of basis sets used in this work.

Name	Basis sets			Size
	Fe	N	H	
	Contracted Gaussian-type orbitals			
A	6-31G*[a]	6-31G*[b]	6-31G**[b]	208
B	TZVP Ahlrichs[c]	TZVP Ahlrichs[c]	TZVP Ahlrichs[c]	255
C	$(8s6p4d2f)$ Wachters[d]	TZVP Ahlrichs[e,c]	TZVP Ahlrichs[e,c]	312
D	$(11s6p5d3f)$ QZVP Ahlrichs[f]	TZVPP Ahlrichs[e,c]	TZVPP Ahlrichs[e,c]	423
	Slater-type orbitals			
A″	DZ[g]	DZ[g]	DZ[g]	137
C″	TZ2P+[g]	TZ2P[g]	TZ2P[g]	457

[a]Reference 44.
[b]Reference 43.
[c]References 52, 81.
[d]References 53, 54.
[e]Polarization exponents taken from TURBOMOLE library.
[f]Reference 55.
[g]Taken from ADF library.

in r_{HS} (0.030 Å) and r_{LS} (0.050 Å) due to differences between the two basis sets.

Figures 5 and 6 summarize the various bond distances obtained for the HS and LS states of $[Fe(H_2O)_6]^{2+}$ and $[Fe(NH_3)_6]^{2+}$ using various methods and basis sets. In the ideal case that Δr_{HL} is independent of the method used for the calculation,

$$r_{HS}=r_{LS}+\Delta r_{HL}. \tag{5.1}$$

This relationship is indeed found for $[Fe(H_2O)_6]^{2+}$ to a remarkably good approximation (Fig. 5). A least-squares fit gives

$$r_{HS}=0.905r_{LS}+0.325\ \text{Å}. \tag{5.2}$$

Figure 6 shows a less strong linear correlation between r_{HS} and r_{LS} for $[Fe(NH_3)_6]^{2+}$, with a least-square fit result,

$$r_{HS}=0.669r_{LS}+0.896\ \text{Å}. \tag{5.3}$$

What is most important is that the overall ordering of points, corresponding to results with different functionals, is roughly the same for $[Fe(H_2O)_6]^{2+}$ and for $[Fe(NH_3)_6]^{2+}$. The two local approximations ($X\alpha$ and LDA) give the shortest bond lengths (both HS and LS). The LDA is known to overbind: bonds tend to be too short. The GGAs correct this and lead generally to a lengthening of the bonds, as observed in the present results. One GGA stands out as giving markedly longer bonds and this is the RPBE functional. Within the cluster of points representing GGAs and hybrids other than the RPBE GGA, the ordering of bond length is very roughly: PW91, PBE, BP86, PBE0<B3LYP*, B3LYP, BLYP<HCTH407, VSXC. The longest bond lengths are observed with the two *ab initio* methods (HF and CASSCF). These latter methods include little electron correlation (none in the case of HF and only a small amount of static correlation in the CASSCF case).

C. Energetics

The HS-LS energy difference is a far more sensitive test of the quality of a density functional than is the structure. As previously mentioned, although experimental data is available indirectly for small compounds such as $[Fe(H_2O)_6]^{2+}$ and $[Fe(NH_3)_6]^{2+}$ through ligand field parameters, we believe that the ability to compare with the results of *ab initio* calculations provides a valuable complement to previous assessments of density functionals for larger compounds.

We thus expect the true value of $\Delta E_{LH}^{\text{adia}}$ for $[Fe(NH_3)_6]^{2+}$ to be in the range 9 000–11 000 cm^{-1}. These results are consistent with the results of the simple LFT model of Figgis and Hitchmann which gives, respectively, 12 000 cm^{-1} and 5 000 cm^{-1} for $\Delta E_{LH}^{\text{adia}}$ for $[Fe(H_2O)_6]^{2+}$ and $[Fe(NH_3)_6]^{2+}$. Thus, in this case, both sophisticated *ab initio* calculations and simple empirical-based LFT calculations basically agree with each other.

Figure 7 and Table V summarizes the results of our DFT calculations of $\Delta E_{LH}^{\text{adia}}$ for $[Fe(H_2O)_6]^{2+}$ and $[Fe(NH_3)_6]^{2+}$. In this bar graph, *ab initio* results are grouped on the left-hand side (LHS) followed by the LFT result, then comes the results for local functionals, followed by GGAs, then HP-

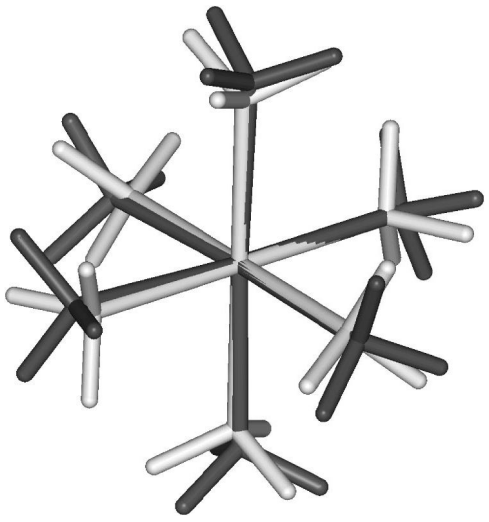

FIG. 3. Superposition of the LS (light) and HS (dark) $[Fe(NH_3)_6]^{2+}$ geometries optimized at the PBE0/*B* level of calculation.

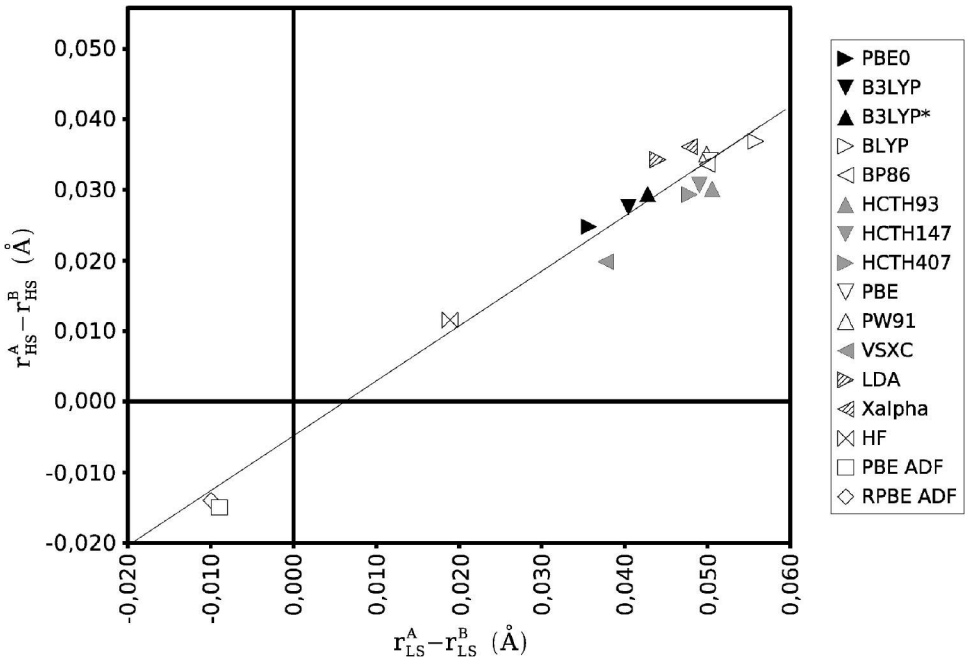

FIG. 4. Comparison of metal-ligand bond length for the high- and low-spin states of $[Fe(NH_3)_6]^{2+}$ with the two basis sets A and B (with the two basis sets A'' and C'' for the ADF calculations).

DFs, and finally on the right-hand side (RHS) are hybrid functionals. For each functional the left (light) bar is for $[Fe(NH_3)_6]^{2+}$ and the right (dark) bar is for $[Fe(H_2O)_6]^{2+}$.

Let us focus first on trends among density functionals. It is remarkable that the $[Fe(NH_3)_6]^{2+}$ DFT bars in Fig. 7 very much resemble a rigid lowering of the $[Fe(H_2O)_6]^{2+}$ DFT bars in Fig. 7. That is, there appear to be definite molecule-independent trends in the values of $\Delta E_{LH}^{\text{adia}}$ calculated with different functionals. The trends for $\Delta E_{LH}^{\text{adia}}$ are roughly: LDA$<X\alpha$, BP86, BLYP, PW91, PBE$<$RPBE, VSXC, PBE0, B3LYP, B3LYP*$<$HCTH407. These are not the same trends observed for Δr_{HL} (LDA, $X\alpha<$PW91, PBE, BP86, PBE0$<$B3LYP*, B3LYP, BLYP$<$HCTH407, VSXC).

Paulsen and Trautwein[10] have found in their calculations on larger spin-crossover compounds that good agreement with experimental (condensed phase) values of $\Delta E_{LH}^{\text{adia}}$ for several ligands could be obtained by a method-dependent, but ligand independent, shift which brings $\Delta E_{LH}^{\text{adia}}$ into agreement with the experimental values for a single choice of ligand. That is,

$$\Delta\Delta E_{LH}^{\text{adia}}(M)=\Delta E_{LH}^{\text{adia}}(L,M)-\Delta E_{LH}^{\text{adia}}(L,X), \tag{5.4}$$

where L represents the choice of ligand, M the computational method, and X the experimental result. It follows that

$$\begin{aligned}\Delta\Delta E_{LH}^{\text{adia}}(L,L')&=\Delta E_{LH}^{\text{adia}}(L,M)-\Delta E_{LH}^{\text{adia}}(L',M)\\&=\Delta E_{LH}^{\text{adia}}(L,X)-\Delta E_{LH}^{\text{adia}}(L',X)\end{aligned} \tag{5.5}$$

should be roughly independent of the choice of computational method. Figure 8 shows that this is indeed roughly the case for different density functionals as long as we exclude the two local approximations. However, as opposed to the

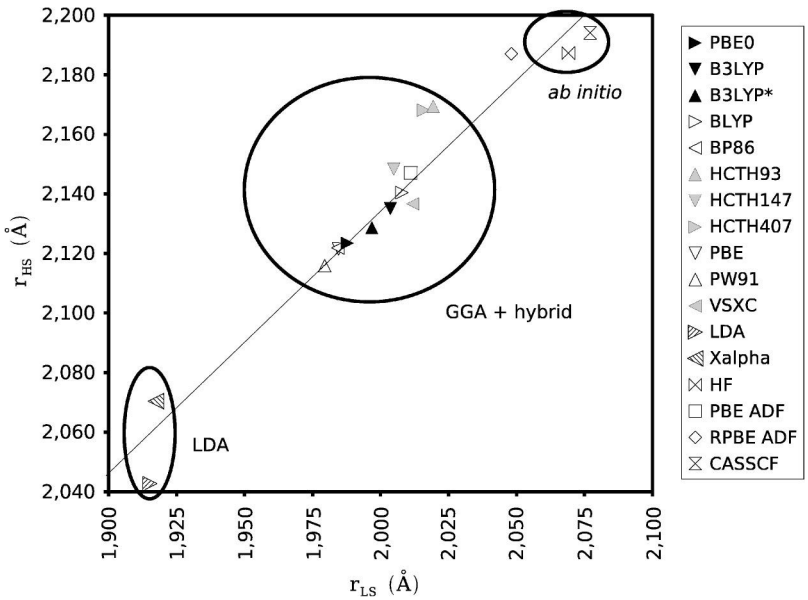

FIG. 5. Comparison of metal-ligand bond length for the high- and low-spin states of $[Fe(H_2O)_6]^{2+}$ with the basis set B (with the basis set C'' for the ADF calculations).

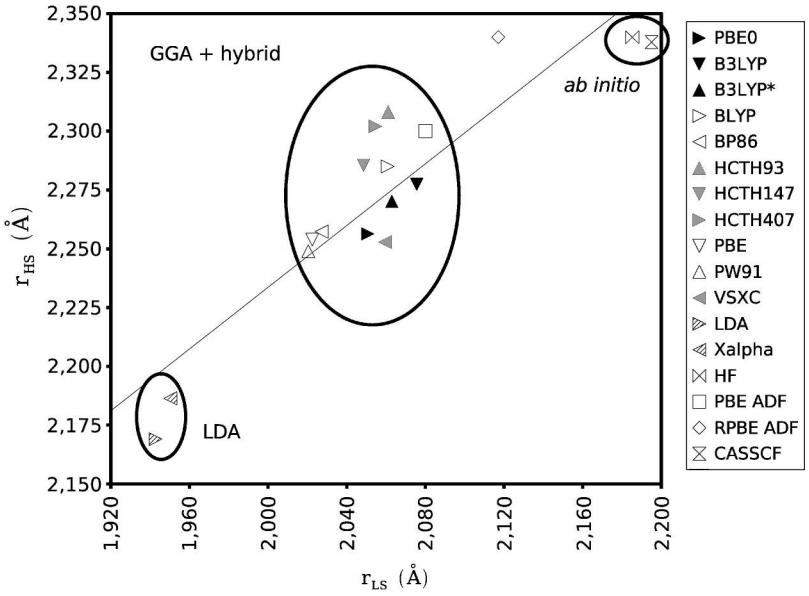

FIG. 6. Comparison of metal-ligand bond length for the high- and low-spin states of $[Fe(NH_3)_6]^{2+}$ with the basis set *B* (with the basis set *C″* for the ADF calculations).

experience of Paulsen and Trautwein,[10] we find that the constant is markedly different than that obtained from our *ab initio* and LFT calculations.

Unlike the case of Δr_{LH} where all the DFT values were too close to each other and to best estimates of the true value, the different DFT values of $\Delta E_{LH}^{\text{adia}}$ differ significantly from our best estimates. We can thus try to assess which is the best functional for estimating this property.

The adiabatic HS-LS energy difference is overestimated at the HF level. Including electron correlation reduces the values, giving our best estimates (labeled CASPT2corr and SORCI). These latter results are reproduced reasonably well by the LFT model. After that comes our DFT results for the two molecules. The LDA seriously underestimates $\Delta E_{LH}^{\text{adia}}$, consistent with the DFT pairing-energy problem which overstabilizes low-spin states with respect to high-spin states. While this underestimation is less severe for traditional GGAs, it is still severe. The RPBE GGA is special in that it gives a larger value of $\Delta E_{LH}^{\text{adia}}$ than the GGAs on its LHS and gives a value of $\Delta E_{LH}^{\text{adia}}$ in reasonable agreement with our best estimate of the true value. The HPDFs on the RHS of the RPBE functional give even larger values of $\Delta E_{LH}^{\text{adia}}$, even exceeding in some cases our best estimate of the true value. The various hybrid functionals give values of which are more or less comparable to those of the HPDFs.

A closer examination (Fig. 7) suggests that the best functionals for $\Delta E_{LH}^{\text{adia}}$ are RPBE, HCTH407, VSXC, B3LYP, PBE0, and B3LYP*, with the best agreement with our best *ab initio* estimates obtained for the VSXC and PBE0 functionals. This is certainly what one might have hoped, namely that the quality of density functionals is increasing with the time and effort spent on generating better functionals (albeit not necessarily monotonically nor without caveats[74]).

VI. CONCLUSION

This paper is a continuation of our work[8] assessing density-functionals for their ability to properly predict changes in molecular geometries and energies associated with a change in spin. This work has been motivated, in particular, by our interest in iron(II) compounds because of their ability to exhibit spin-crossover phenomena making them interesting case studies for solid state molecular optical switches.[3] Molecular switches[75] are, of course, highly interesting because of the present international interest in developing nanotechnology. In particular, spin-crossover phenomena in transition metal compounds is the subject of three recent volumes of the series *Topics in Current Chemistry*.[1] Nevertheless the ability of density-functionals to properly treat different spin states is by no means limited to material science as has been nicely emphasized in a recent review on chemical reactivity by Harvey.[9]

Previous work aimed at assessing density functionals for the treatment of spin-crossover phenomena focused on larger compounds and test data obtained from condensed matter experiments.[4–7,10] Although highly valuable, we feel that this work can be clouded by the difficulties of comparing gas phase computed values with condensed phase experimental values for compounds such as these where environmental effects are known to be highly significant.[3,27] That is why we

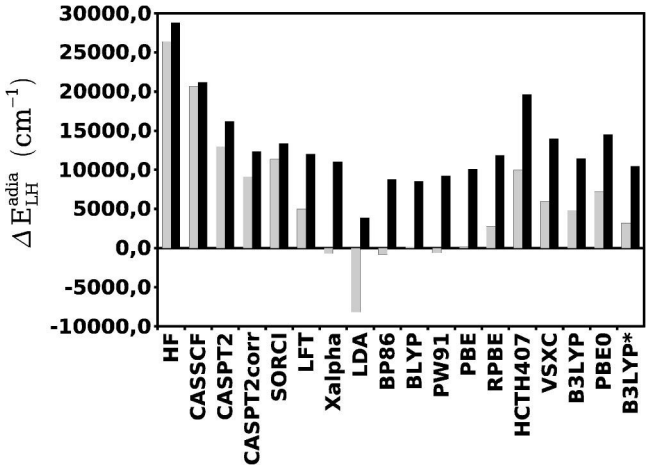

FIG. 7. $\Delta E_{LH}^{\text{adia}}$ for $[Fe(H_2O)_6]^{2+}$ (dark bar) and $[Fe(NH_3)_6]^{2+}$ (light bar).

TABLE V. $[Fe(NH_3)_6]^{2+}$ and $[Fe(H_2O)_6]^{2+}$ HS-LS energy differences.

Method	HS-LS energy differences (cm^{-1}) $[Fe(NH_3)_6]^{2+}$	$[Fe(H_2O)_6]^{2+}$
	MOLCAS[a]	
CASSCF(12,10)	20 630/16 792	21 180/17 892[b]
CASPT2(12,10)	12 963/9125	16 185/12 347[b]
	ORCA	
SORCI/*C*	10 390[c]	13 360[b]
SORCI/*D*	11 250[c]	
	LFT	
LFT	5000	12 000
	GAUSSIAN	
Xα/*A*	−1238	11 280[b]
Xα/*B*	−695	11 040[b]
VWN/*A*	−8817	3316[b]
VWN/*B*	−8187	3896[b]
BP86/*A*	−241	8985[b]
BP86/*B*	−790	8798[b]
BLYP/*A*	488	8564[b]
BLYP/*B*	161	8548[b]
PW91/*A*	−299	9271[b]
PW91/*B*	−617	9232[b]
PBE/*A*	581	10 181[b]
PBE/*B*	147	10 081[b]
HCTH93/*A*	10 299	19 062
HCTH93/*B*	9430	18 779
HCTH147/*A*	9344	18 435
HCTH147/*B*	8576	18 211
HCTH407/*A*	10 682	19 789
HCTH407/*B*	9962	19 631
VSXC/*A*	6991	14 860
VSXC/*B*	5928	13 975
B3LYP*/*A*	3651	10 519
B3LYP*/*B*	3226	10 456
B3LYP/*A*	5260	11 514[b]
B3LYP/*B*	4978	11 465[b]
PBE0/*A*	7799	14 676
PBE0/*B*	7195	14 504
HF/*A*	25 667	27 627
HF/*B*	26 381	28 796
	ADF	
PBE/*A″*	−498	
PBE/*C″*	−640	9056[b]
RPBE/*A″*	2911	
RPBE/*C″*	2744	11 844[b]

[a]The notation *X*/*Y* indicates (*Y*) and without (*X*) atomic corrections from Ref. 8.
[b]Reference 8.
[c]Geometries relaxation energy obtained from B3LYP/TZVP calculations.

have chosen to focus, in the first instance, upon small compounds such as $[Fe(H_2O)_6]^{2+}$ and $[Fe(NH_3)_6]^{2+}$. The drawback of this approach is that very little experimental data is available for these compounds and so our primary comparison has been with the results of our own CASPT2 and SORCI calculations which we believe to be among the best in the literature for these compounds. In addition, it is interesting to note that they agree reasonably well with the results of a simple empirically based LFT calculation.

In paper I,[8] we reported our *ab initio* calculations for $[Fe(H_2O)_6]^{2+}$ as well as calculations using the density functionals *Xα*, LDA, BP86, BLYP, PW91, B3LYP, PBE, and RPBE. Previous work had pointed out the existence of what might be called the "density-functional theory pairing-energy problem" where the LDA overstabilizes low-spin states relative to high-spin states (see Ref. 8 for a thorough discussion). This problem is reduced but not eliminated by the GGAs BP86, BLYP, PW91, and PBE. We did however show that it is largely corrected for $[Fe(H_2O)_6]^{2+}$ by the RPBE and B3LYP functionals.[8] Since then other highly parametrized density functionals (HPDFs) have become more widely available, making it interesting to extend the assessment of paper I to the HCTH family of functionals (HCTH93, HCTH147, and HCTH407), the VSXC functional, as well as the hybrid functional PBE0. In all, 13 functionals have now been evaluated for spin-state dependent changes in the geometry and total energy of $[Fe(H_2O)_6]^{2+}$. We also wanted to extend our study to at least one other molecule, which we have done here in the case of $[Fe(NH_3)_6]^{2+}$.

We find definite and distinct trends in the ability of different functionals to treat these complexes. All GGAs and hybrid functionals appear to do an acceptable job of treating changes in the geometries of these coordination complexes. Trends in Δr_{HL} are

$$\Delta r_{HL}: \text{HCTH407, } X\alpha > \text{LDA, PW91, PBE, BP86,}$$
$$\text{RPBE} > \text{BLYP, PBE0, B3LYP*, B3LYP} > \text{VSXC.}$$

This is not the same trends observed in $\Delta E_{HL}^{\text{adia}}$,

$$\Delta E_{HL}^{\text{adia}}: \text{LDA} < X\alpha, \text{ BP86, BLYP, PW91,}$$
$$\text{PBE} < \text{B3LYP*, RPBE, VSXC, B3LYP,}$$
$$\text{PBE0} < \text{HCTH407.}$$

Since our *ab initio* calculations provide best estimates of $\Delta E_{HL}^{\text{adia}}$, we are able to say with some confidence that the VSXC and PBE0 functionals (among functionals tested here) are the best functionals for calculating the adiabatic HS-LS energy difference in $[Fe(H_2O)_6]^{2+}$ and $[Fe(NH_3)_6]^{2+}$, though B3LYP, B3LYP*, RPBE, and HCTH407 are also quite good.

Although these results are encouraging, it may be useful to end on a note of caution. Since $[Fe(H_2O)_6]^{2+}$ and $[Fe(NH_3)_6]^{2+}$ are quite simple model compounds one should question their usefulness when trying to understand more complicated spin-crossover systems. Antolovic and Davidson[76] have suggested that dispersion forces are needed in the quantitative description of coordination bonding and DFT is commonly believed to severely underestimate dispersion forces. If dispersion forces are really needed for a quantitative description of coordination bonding, we may be getting "the right answer for the wrong reason," in which case extrapolation to the case of true spin-crossover complexes may or may not be possible. We are thus looking forward with some excitement to see what happens as we extend our investigations to larger compounds which better reflect spin-crossover chemistry. We are in the course of carrying out such tests.

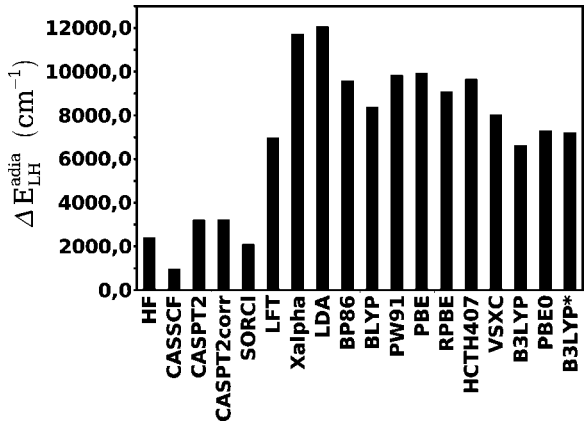

FIG. 8. Difference of $\Delta E_{LH}^{\text{adia}}$ between $[Fe(H_2O)_6]^{2+}$ and $[Fe(NH_3)_6]^{2+}$ with the basis set *B*.

ACKNOWLEDGMENTS

This study was carried out in the context of the *groupe de recherche en Commutateurs Optiques Moléculaires à l'Etat Solide* (COMES), *groupe de recherche en density-functional theory* (DFT) and the working group COST D26/0013/02. A.F. would like to acknowledge the French *Ministère d'Education* for a *Bourse de Mobilité*. M.E.C. and A.F. would like to thank Pierre Vatton, Denis Charapoff, Marie-Louise Dheu-Andries, and Régis Gras for technical support of the LEDSS and *Center d'Expérimentation pour le Calcul Intensif en Chimie* (CECIC) computers used for many of the calculations reported here and would also like to acknowledge supercomputer time at the *Institut du Développement et des Ressources en Informatique Scientifique* (IDRIS) in the context of IDRIS project No. 021576. The authors would like to thank Carlo Adamo for helpful discussions. A.H. and L.M.L.D. acknowledge supercomputer time at the *Centro Svizzero di Calcolo Scientifivo* (CSCS) in the framework of the CSCS project entitled "Photophysics and Photochemistry of Transition Metal Compounds: Theoretical Approaches." F.N. acknowledges the Deutsche Forschungsgemeinschaft for financial support within the priority program 1137 "Molecular Magnetism."

[1] *Spin Crossover in Transition Metal Complexes I*, Topics in Current Chemistry Vol. 233, edited by P. Gütlich and H. A. Goodwin (Springer, Berlin, 2004); *Spin Crossover in Transition Metal Complexes II*, Topics in Current Chemistry Vol. 234, edited by P. Gütlich and H. A. Goodwin (Springer, Berlin, 2004); *Spin Crossover in Transition Metal Complexes III*, Topics in Current Chemistry Vol. 235, edited by P. Gütlich and H. A. Goodwin (Springer, Berlin, 2004).
[2] H. A. Goodwin, Coord. Chem. Rev. **18**, 293 (1976).
[3] P. Gütlich, A. Hauser, and H. Spiering, Angew. Chem., Int. Ed. Engl. **33**, 2024 (1994).
[4] H. Paulsen, L. Duelund, H. Winkler, H. Toftlund, and A. X. Trautwein, Inorg. Chem. **40**, 2201 (2001).
[5] M. Reiher, O. Salomon, and B. A. Hess, Theor. Chem. Acc. **107**, 48 (2001).
[6] O. Salomon, M. Reiher, and B. A. Hess, J. Chem. Phys. **117**, 4729 (2002).
[7] M. Reiher, Inorg. Chem. **41**, 6928 (2002).
[8] A. Fouqueau, S. Mer, M. E. Casida, L. M. Lawson Daku, A. Hauser, T. Mineva, and F. Neese, J. Chem. Phys. **120**, 9473 (2004).
[9] J. N. Harvey, in *Principles and Applications of Density Functional Theory in Inorganic Chemistry I, Structure and Bonding* Vol. 112, edited by N. Kaitsoyannis and J. E. McGrady (Springer-Verlag, Heidelberg, 2004), p. 151.
[10] H. Paulsen and A. X. Trautwein, J. Phys. Chem. Sol. **65**, 793 (2004).
[11] W. Kohn and L. J. Sham, Phys. Rev. **140**, A1133 (1965).
[12] O. Gunnarson and B. I. Lundqvist, Phys. Rev. B **13**, 4274 (1976).
[13] S. H. Vosko, L. Wilk, and M. Nusair, Can. J. Phys. **58**, 1200 (1980).
[14] R. M. Dreizler and E. K. U. Gross, *Density Functional Theory: An Application to the Quantum Many-Body Problem* (Springer, Berlin, 1990).
[15] J. K. Labanowski and J. W. Andzelm, *Density Functional Methods in Chemistry*, (Springer, New-York, 1991).
[16] I. N. Levine, *Quantum Chemistry*, 5th ed. (Prentice-Hall, Upper Saddle River, NJ, 2000).
[17] A. D. Becke, Phys. Rev. B **38**, 3098 (1988).
[18] C. Lee, W. Yang, and R. G. Parr, Phys. Rev. B **38**, 3098 (1988).
[19] A. D. Becke, J. Chem. Phys. **98**, 1372 (1993).
[20] J. Harris and R. O. Jones, J. Phys. F: Met. Phys. **4**, 1170 (1974).
[21] A. D. Becke, J. Chem. Phys. **98**, 5648 (1993).
[22] Gaussian Incorporated NEWS, v. 5, Wallingford, Connecticut 06492, 1994.
[23] J. P. Perdew, M. Ernzerhof, and K. Burke, J. Chem. Phys. **105**, 9982 (1996).
[24] C. Adamo and V. Barone, J. Chem. Phys. **110**, 6158 (1999).
[25] U. Salzner, J. B. Lagowski, P. G. Pickup, and R. A. Poirier, J. Phys. Chem. A **102**, 2572 (1998).
[26] P. J. Xilson, R. D. Amos, and N. C. Handy, Chem. Phys. Lett. **312**, 475 (1999).
[27] M. Hosteller, K. W. Törnroos, D. Chernyshov, and H. B. Börgi, 21st European Cristallographic Meeting, Durban, South Africa, 24-29 August 2003, Abstract f4.m8.04, p. 88.
[28] T. V. Voorhis and G. E. Scuseria, Mol. Phys. **92**, 601 (1997).
[29] T. V. Voorhis and G. E. Scuseria, J. Chem. Phys. **109**, 400 (1998).
[30] F. A. Hamprecht, A. J. Cohen, D. J. Tozer, and N. C. Handy, J. Chem. Phys. **109**, 6264 (1998).
[31] B. N. Figgis and M. A. Hitchman, *Ligand Field Theory and Its Applications* (Wiley-VCH, New York, 2000).
[32] S. Sugano, Y. Tanabe, and H. Kamimura, *Multiplets of Transition-Metal Ions in Crystals* Pure and Applied Physics Vol. 33, edited by H. S. W. Massey and K. A. Brueckner (Academic, New York, 1970).
[33] J. S. Griffith, *The Theory of Transition Metal Ions* (Cambridge University Press, Cambridge, 1961).
[34] M. Brorson and C. E. Schäffer, Inorg. Chem. **27**, 2522 (1988).
[35] B. O. Roos, P. R. Taylor, and P. E. M. Siegbahn, Chem. Phys. **48**, 157 (1980).
[36] K. Andersson, P.-Å. Malmqvist, B. O. Roos, A. J. Sadlej, and K. Wolinski, J. Phys. Chem. **94**, 5483 (1990).
[37] K. Andersson, P.-Å. Malmqvist, and B. O. Roos, J. Phys. Chem. **96**, 1218 (1992).
[38] F. Neese, J. Chem. Phys. **119**, 9428 (2003).
[39] J. Miralles, O. Castell, R. Caballol, and J.-P. Malrieu, Chem. Phys. **172**, 33 (1993).
[40] J. Miralles, J.-P. Daudey, and R. Caballol, Chem. Phys. Lett. **198**, 555 (1992).
[41] B. O. Roos, K. Andersson, M. P. Fuelscher, P.-Å. Malmqvist, L. S. Andres, K. Pierloot, and M. Manuela, Adv. Chem. Phys. **93**, 219 (1996).
[42] K. Andersson, M. Barysz, A. Bernhardsson *et al.*, MOLCAS, Version 5, Lund University, Sweden, 2000.
[43] P. C. Hariharan and J. A. Pople, Theor. Chim. Acta **28**, 213 (1973).
[44] V. Rassolov, J. A. Pople, M. Ratner, and T. L. Windus, J. Chem. Phys. **109**, 1223 (1998).
[45] C. Froese-Fischer, J. Phys. B **10**, 1241 (1977).
[46] T. H. Dunning, Jr., B. H. Botch, and J. F. Harrisson, J. Chem. Phys. **72**, 3419 (1980).
[47] B. H. Botch, T. H. Dunning, Jr., and J. F. Harrisson, J. Chem. Phys. **75**, 3466 (1981).
[48] R. Åkesson, L. G. M. Pettersson, M. Sandström, and U. Wahlgren, J. Am. Chem. Soc. **116**, 8691 (1994).
[49] C. W. Bauschlicher, Jr., in *Modern Electronic Structure theory, Part II* edited by D. R. Yarkony (World Scientific, Singapore, 1995).
[50] P. E. M. Siegbahn, Adv. Chem. Phys. **93**, 333 (1996).
[51] F. Neese, ORCA- an *ab initio*, density functional and Semiempirical Program Package, Version 2.4.16, Max-Planck Institut für Bioanorganische Chemie, Mülheim, Germany, 2004.
[52] A. Schäfer, C. Huber, and R. Ahlrichs, J. Chem. Phys. **100**, 5829 (1994).
[53] A. J. H. Wachters, J. Chem. Phys. **52**, 1033 (1970).
[54] C. W. Bauschlicher, Jr., S. R. Langhoff, and L. A. Barnes, J. Chem. Phys. **91**, 2399 (1989).

[55] F. Weigend, F. Furche, and R. Ahlrichs, J. Chem. Phys. **119**, 12753 (2003).
[56] F. Weigend, A. Kohn, and C. Hattig, J. Chem. Phys. **116**, 3175 (2002).
[57] K. K. Stavrev and M. C. Zerner, Int. J. Quantum Chem. **65**, 877 (1997).
[58] B. J. Mogensen and S. Rettrup, Int. J. Quantum Chem. **44**, 1045 (1992).
[59] S. Grimme and M. Waletzke, Phys.Chem.Chem.Phys. **111**, 5845 (1999).
[60] K. Andersson, Theor. Chim. Acta **91**, 31 (1995).
[61] G. Hirsch, P. J. Bruna, S. D. Peyerimhoff, and R. J. Buenker, Chem. Phys. Lett. **52**, 442 (1977).
[62] P. J. Bruna, S. D. Peyerimhoff, and R. J. Buenker, Chem. Phys. Lett. **72**, 278 (1980).
[63] P. A. M. Dirac, Proc. Cambridge Philos. Soc. **26**, 376 (1930).
[64] J. C. Slater, Phys. Rev. **81**, 385 (1951).
[65] J. A. Pople, M. Head-Gordon, D. J. Fox, K. Raghavachari, and L. A. Curtiss, J. Chem. Phys. **90**, 5622 (1989).
[66] L. A. Curtiss, C. Jones, G. W. Trucks, K. Raghavachari, and J. A. Pople, J. Chem. Phys. **93**, 2537 (1990).
[67] L. A. Curtiss, K. Raghavachari, G. W. Trucks, and J. A. Pople, J. Chem. Phys. **94**, 7221 (1991).
[68] L. A. Curtiss, K. Raghavachari, P. C. Redfern, V. Rassolov, and J. A. Pople, J. Chem. Phys. **109**, 7764 (1998).
[69] M. J. Frisch, G. W. Trucks, H. B. Schlegel *et al.*, GAUSSIAN03, Revision A.1, Gaussian, Inc., Pittsburgh, PA, 2003.
[70] AMSTERDAM DENSITY FUNCTIONAL Program, Theoretical Chemistry, Vrije Universiteit, Amsterdam, the Netherlands, http://www.scm.com.
[71] M. J. Frisch, G. W. Trucks, H. B. Schlegel, G. E. Scuseria *et al.*, GAUSSIAN98, Revision A.7, Gaussian Inc., Pittsburgh, PA, 1998.
[72] E. Cancès, J. Chem. Phys. **114**, 10616 (2001).
[73] K. N. Kudin, G. E. Scuseria, and E. Cancès, J. Chem. Phys. **116**, 8255 (2002).
[74] R. Ahlrichs, F. Furche, and S. Grimme, Chem. Phys. Lett. **325**, 317 (2000).
[75] B. L. Feringa, *Molecular Switches* (Wiley-VCH, Weinheim, 2001).
[76] D. Antolovic and E. R. Davidson, J. Chem. Phys. **88**, 4967 (1988).
[77] J. P. Perdew, Phys. Rev. B **33**, 8822 (1986).
[78] J. P. Perdew, K. Burke, and Y. Wang, Phys. Rev. B **54**, 16533 (1996).
[79] B. Hammer, L. B. Hansen, and J. K. Nørskov, Phys. Rev. B **59**, 7413 (1999).
[80] K. Nakamoto, *Infrared and Raman Spectra of Inorganic and Coordination Compounds* (Wiley-Intersciences, New York, 1997).
[81] A. Schäfer, H. Horn, and R. Ahlrichs, J. Chem. Phys. **97**, 2571 (1992).